Journal of Chemical Technology and Metallurgy, 58, 6, 2023, 1153-1162

ON THE MECHANICAL BEHAVIOUR OF THERMALLY AFFECTED NON-HEAT-TREATABLE ALUMINIUM ALLOYS

Nasim Rokon[1], Mohammad Salman Haque[2], Mohammad Salim Kaiser[3]

[1]Department of Materials Science and Engineering
Rajshahi University of Engineering & Technology
Rajshahi, Bangladesh
[2] Department of Materials Science and Engineering
Khulna University of Engineering & Technology, Khulna, Bangladesh
[3] Innovation Centre
International University of Business Agriculture and Technology
Dhaka, Bangladesh
E-mail: dkaiser.res@iubat.edu

Received 22 December 2022
Accepted 20 March 2023

ABSTRACT

The influence of heat treatment on the mechanical behavior in terms of true stress-strain and mode of fracture of the deferent non-heat-treatable alloys has been carried out. Hardness, resistivity and the microstructural change of the alloys due to annealing also consider for complying the properties. In this purpose the hot rolled followed by cold rolled alloys samples are isochronally annealed for one hour at different temperatures. The experimental results show that maximum strength can be achieved by 5xxx series alloys followed by 3xxx, 4xxx and the lowest for 1xxx series alloys as attributed to the alloying element performance. Increasing of heat treatment temperature led to decrease in hardness and resistivity of the alloys by reason of recovery and coarsened the grains. The stress-strain curves show the lower strength and higher elongation with annealing temperature. Microstructural study also confirms that cold rolled alloys contents the elongated grain but annealing at 400°C per one hour a recrystallized grains are formed. Fractographic observations also verify that commercially pure aluminum and silicon added alloys are fractured of ductile mechanism, but manganese and magnesium added alloys demonstrate a brittle type of fracture as by reason of formed intermetallic phases.

Keywords: Al-alloys, hardness, resistivity, true stress-strain, microstructure, fracture.

INTRODUCTION

Based on heat treatment, there are two basic types of aluminum alloys in practical application namely heat-treatable and non-heat-treatable alloys [1, 2]. The primary strength of heat-treatable alloys is created by alloying elements which form various intermetallics in the Al matrix. Mostly used alloying elements are copper, magnesium, silicon and lithium/tin. Depending on these elements, the alloys are also termed as 2xxx series, 6xxx series, 7xxx and 8xxx series Al-alloys respectively [3, 4]. Since these elements in various combinations show increasing solid solubility in aluminum with increasing temperature, it is possible to subject them to thermal treatments that will impart pronounced strengthening. This method involves a sequence of solution heat treatment, subsequent quenching, and then precipitation hardening or age hardening [5]. Maximum strength can be achieved by proper combination of these heat treatments. Besides, strength of non-heat-treatable alloys are created through solid solution strengthening, where pure aluminum, manganese, silicon, and magnesium are the alloying elements. These are designated as the 1xxx, 3xxx, 4xxx, and 5xxx series, respectively [3, 6]. Various levels of cold working or strain hardening are employed to increase the additional strength of such alloys. Plastic deformation is performed by rolling, dies or similar operations where the area is reduced. The level of area

reduction controls the material ultimate properties [7].

Aluminum alloys are used in a wide variety of applications in the automobile, marine and aerospace industries for their low specific gravity, high strength to weight ratio, high wear resistance, high reflectivity, excellent heat and electrical conductivity, low melting point, negligible gas solubility, excellent castability and good corrosion resistance [8 - 10]. A new type of aluminum alloy material has emerged in recent years that is non-heat-treated aluminum alloy. The advantages of these alloys are that the material does not have to undergo solution treatment at high temperatures as well as artificial aging. Aluminum alloys can achieve high strength through natural aging only to satisfy the high performance for automobile and aerospace apparatuses [11 - 13].

After a literature review, it is clear that there are few research reports on non-heat-treated aluminum alloys, including very few reports on high-strength, high-plasticity, non-heat-treated aluminum alloys. The study also confirms that rolling reduction and the following annealing temperature are two important parameters for safely used of the non-heat treatable alloys [14, 15]. Therefore, it is very necessary to study the effects of rolling reduction and annealing temperature on microstructure and mechanical properties of these alloys. Therefore, the effect of annealing temperature on the hardness, precipitated behavior, mechanical properties, metallographic structure and fracture morphology of different non-heat treatable wrought alloys were studied. The reasonable annealing temperature was determined for consideration of the factor of safety in actual engineering design.

EXPERIMENTAL

The required melting was done in a gas fired pit furnace under a flux cover such as degasser, borax, etc. Commercially pure aluminum was taken as the starting material to prepare the alloy. To cast the alloys, aluminum was first melted in a clay-graphite crucible and then alloying elements such as commercially pure magnesium, Al-Si (50 % Si) master alloy were added by dipping into the molten metal. Mn-Al (80 % Mn) alloy powder was taken in an aluminum foil cover and then added by dipping. During the melting temperature of the furnace was always maintained at 780 ± 15°C with the help of the electronic controller. Then the melt was homogenized under stirring at 700°C and poured in 200°C preheated 18.0 mm x 125.0 mm x 250.0 mm cast iron metal mould. Four alloys chemical compositions were analyzed by optical emission spectroscopy (OES) methods and the main elements are in Table 1. Furthermore, Cr, Zn, Ni, Pb, Sn, etc., were also present as trace impurities.

Table. 1. Chemical composition of the experimental alloys (wt. %).

Al alloy	Si	Mn	Mg	Fe	Al
1xxx	0.327	0.002	0.004	0.290	Bal
3xxx	0.486	2.565	0.006	0.326	Bal
4xxx	3.032	0.006	0.014	0.207	Bal
5xxx	0.356	0.009	3.100	0.899	Bal

Four cast alloys were homogenized for a time duration of 6 hours at 400°C and then cooled slowly inside furnace. Solutionizing treatment was conducted for 2 hours at 530°C followed by rapid cooling in water.

For the rolling operation alloys were machined in a size of 20 x 17 x 250 mm. First the samples were deformed to a thickness of 15 x 17 x 250 mm by hot rolling maintaining the temperature at 400°C followed by 80 % cold rolling which reduced the thickness from 15 mm thick to 3.0 mm. In this case the deformation for each pass was about 1.0 mm. Both hot and cold rolling were done with a laboratory scale rolling mill of 10HP capacity. Sample for hardness and conductivity measurement 3 x 15 x 15 mm in size were obtained from the cold rolled samples. The samples were annealed for a period of 60 minutes at various temperatures up to 400°C to study the effect of heat treatment. The hardness of the machined surface was also taken using a Rockwell Brinell hardness testing machine named Zwick hardness tester where 1/8-inch ball in B scale was used. Tensile testing was performed according to ASTM specifications using an Instron testing machine at room temperature. The gauge length of the tensile specimen was 25 mm and the sustaining strain rate was 10^{-3}/s. Five tests were undertaken at each condition and the closest value of the average of the results is used to build the true stress-strain curve. Impact test was also carried out following ASTM standards with 2 mm deep 45° angle V-shaped grooves with specimen size of 10 x 10 x 55 mm. Electrical conductivity of the alloys was

carried out with an Electric Conductivity Meter, type 979. 15 mm x 15 mm finished surface samples produced by grinding and polishing were prepared for this measurement. Electric resistivity was calculated from those conductivity data. The optical metallography of all these samples was carried out in the usual way where Inverted Metallurgical Microscope was employed. The specimens were prepared through a conventional mechanical polishing finally with alumina followed by etching with Keller reagent. After the tensile test the fracture surfaces were examined by a Jeol Scanning Electron Microscope type of JSM-5200.

RESULTS AND DISCUSSION

Isochronal annealing

Fig. 1 illustrates the results of isochronal annealing on hot rolled and 80 % cold-worked alloys at different temperatures for one hour. It has been observed that almost all alloys are initially softened by this of dislocation rearrangement and grain recovery inside the cold deformed alloys followed by another softening for particle coarsening and recrystallization at higher annealing temperature. The rate of softening varies on the alloy's composition, although Mg-added alloys softened significantly when annealed at high temperatures compared to other alloys. Binary phase diagram of Al-Mg shows that the dissolution temperature of Al_3Mg_2 in the alloy matrix around at 250°C so the Mg-added Al alloy's hardness dramatically dropped as the brittle phase dissolved [16]. This caused the Mg alloy to soften faster than the other alloys being exposed to higher temperatures. Similarly, Al-Mn binary phase diagram indicates that the brittle $Al_{12}Mn$ phase is stable up to 450°C [17]. As a result, at higher temperatures the rate of softening was much relatively low compared that of other alloys. In case of Si in Al alloy, the binary phase diagram indicates the presence of eutectic Si within the aluminium matrix, and yet no intermetallic compounds between Si and Al is developed. It also confirms that the spherical Si can be clearly seen in the scanning electron micrograph image [18]. Because of this, the level of softening is substantially more than in an aluminum alloy with manganese added.

Fig. 2 indicates the variation of average values of electric resistivity of the experimental non-heat treatable alloys with annealing temperature. The electrical resistivity of the 3xxx, 4xxx and 5xxx series alloys demonstrate the higher values than of commercially pure 1xxx alloy. Alloying may disturb the crystal lattice, which slows down or inhibits electrons as they flow through the material [19]. The formation of Al_3Mg_2 and

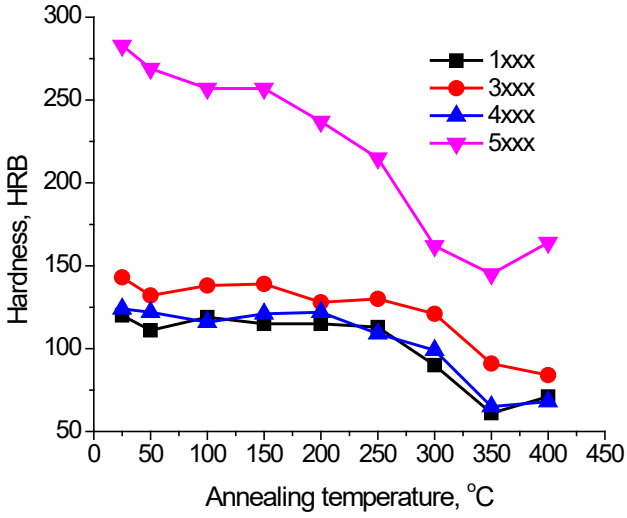

Fig. 1. Isochronal annealing curve of the 80 % cold rolled alloys for 1 hour.

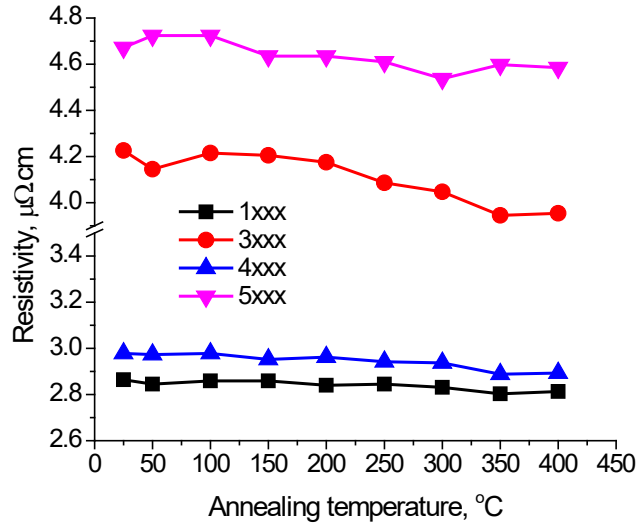

Fig. 2. Variation of resistivity due to isochronal annealing of the 80 % cold rolled alloys for 1 hour.

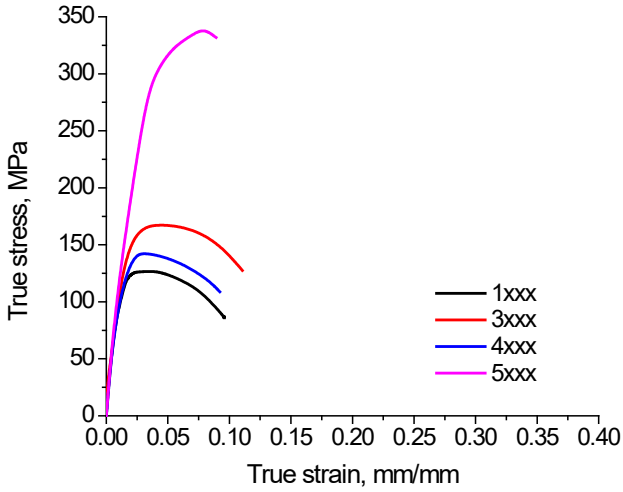

Fig. 3. True stress - true strain curve for the alloys as rolled condition at room temperature.

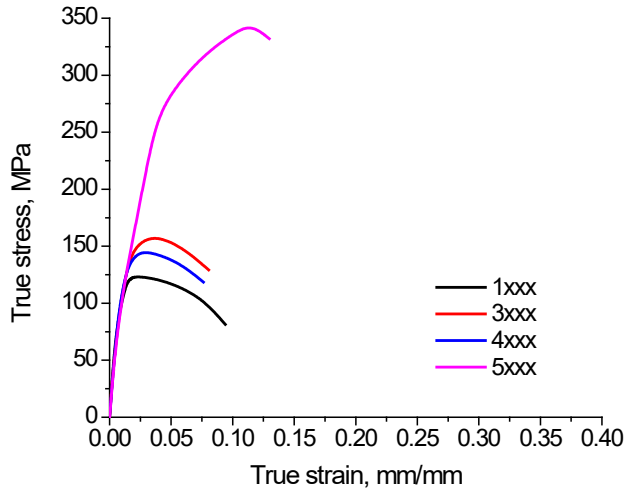

Fig. 4. True stress - true strain curve for the alloys annealed at 150°C for one hour.

Al_8Mg_5 intermetallic compounds increases electrical resistivity, despite Mg's lower value compared to Mn or Si. Rolling deposits corroded particles at the grain boundary, which impedes electron mobility across the alloy. Therefore, the addition of Mg to the Al alloy resulted in a rise in electrical resistivity. When Mn is added, Al_6Mn form during solidification and during annealing the brittle intermetallic phase $Al_{12}Mn$ is also responsible for the rise in electrical resistivity. The free mobility of electrons is not hindered by the presence of eutectic Si in the Al matrix because of its spherical form. As a result, its electrical resistance is much lower compared to that of other alloys.

From the figure described the resistivity drop at initial stage during isochronal annealing of the four non-heat treated alloys are associated with minimize or rearrangement of dislocation and vacancies as the said alloys are heavily work hardened. Some deviation is observed at the intermediate stage of annealing because of fine precipitates take place through GP zones and metastable phase formation. The presence of different elements into different alloy controls the formation of precipitation temperature. These precipitates barricade the dislocation movement thus the higher resistivity. At the higher annealing temperature resistivity reduction occurs through recovery, particle coarsening as well as recrystallization as make smaller the scattering centers [10].

True stress true strain

Figs. 3, 4, and 5 illustrate the true stress-strain curves derived from the tensile test outcomes of the experimental alloys when the alloys were annealed at room temperature, 150°C, and 400°C for one hour, respectively. In the true stress-strain curve of room temperature, except the tensile strength, more or less identical elongation is evident (Fig. 3) [20]. Hot rolled followed by heavily cold rolled alloys consists of considerably elongated grains and sub-grains along with lots of dislocations surrounded which further hinders dislocations slip. Thus, deeply deformed results in the increase of tensile strength and reduce of elongation percentage. Pure aluminium is a rather ductile material. The yield strength of 80 % cold-rolled pure aluminium is found around 120 MPa. However, the yield strength improved once alloying elements like Mn, Si, and Mg were introduced. However, the production of Al_3Mg_2 once Mg was added nearly tripled the yield strength though the elongation has been reduced. $Al_{12}Mn$ intermetallic phase was formed in the aluminium alloy due to Mn addition in 3xxx, making the alloy brittle. This resulted in an increase in the pure aluminium's yield strength, but it also led to a decrease in the material's elongation. Because Si could not form an intermetallic compound with the aluminium, it had a negligible effect on the alloy's yield strength and elongation. Even though, the yield strength is slightly improved because

of eutectic globular Si.

The true stress-strain curve under annealed at 150°C for one hour exhibit a similar nature to that observed at room temperature (Fig.4). Here a small variation is observed in both the strength and elongation contributed by two differing effects. Annealing treatment reduces vacancies and dislocation density as a result reduction of tensile strength and improvement of elongation. On the other hand, formation of precipitates through GP zones and metastable phases result improvement of tensile strength and reduction of elongation [21, 22]. Reduction of dislocation density has an effect as a slight decline in the curves.

The true stress - strain diagram of aluminium alloy after they have been annealed at 400°C for 1 hour is depicted in Fig. 5. After being annealed at a high temperature, the alloy experiences a considerable decrease in its yield strength. Aluminum alloys in general soften as a result of grain coarsening. Elongation, on the other hand, has been greatly enhanced throughout the entire alloy. This indicates that the cold rolled effect, which is the cause of the brittleness in the alloy, has been removed. The ductile properties of the alloy are manifested throughout. When compared to its alloy, pure aluminum shows the greatest elongation. The loss of ductility is traced back to cold rolling alone for pure aluminum. However, the stresses caused by the rolling process are eliminated by subjecting the aluminum to annealing process at a higher temperature [23, 24]. Further, grain coarsening occurs, which aids in the progress toward greater elongation. The intermetallic compounds in the alloy, which together with the cold rolling produced the brittle phase, were dissolved at higher temperatures. At 400°C for one hour, the eutectic, brittle globular Si, $Al_{12}Mn$ and Al_3Mg_2 intermetallics are dissolved, transforming the brittle alloy into the ductile one. The elongation of the alloys also improves significantly at higher temperature by dissolving the intermetallic phase. It is well established that precipitates perform as a barrier to dislocation movement so in this overaged condition under lower barrier a clear decline nature stress-strain curves are observed for all the alloys.

Impact energy

The experimental results of the impact energy of the differently processed work harden alloys are plotted in Fig. 6. At the entire conditions 1xxx series alloy shows the highest energy due to the purity of aluminum. Brittle natures of compound are generated in 3xxx and 5xxx alloys when Mg and Mn are introduced, whereas eutectic globular Si formed in 4xxx alloy when Si is added in to Al-alloy. These compounds are responsible for the subsequent lowering the toughness of the material [25]. The 5xxx series alloy exhibits the lowest energy as the

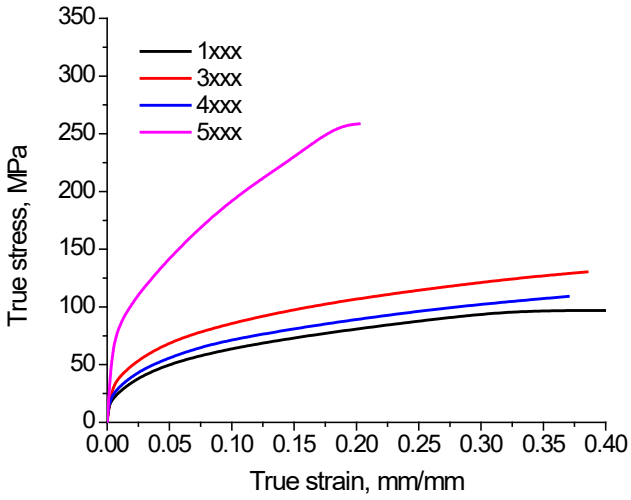

Fig. 5. True stress - true strain curve for the alloys annealed at 400°C for one hour.

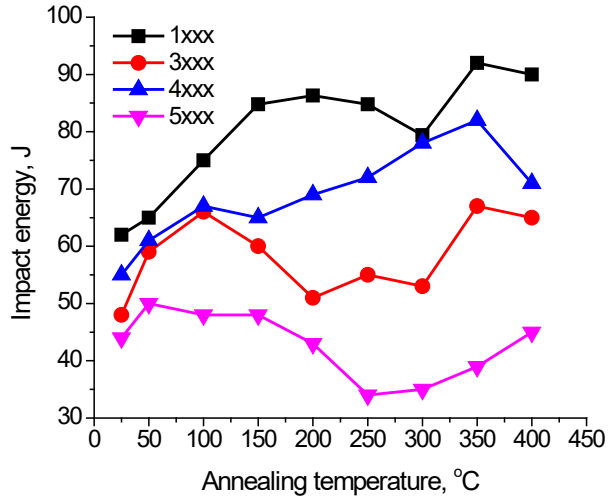

Fig. 6. Variation of impact energy of the experimental alloys isochronally annealed at different temperature for one hour.

formed Mg-rich intermetallics commence the stress corrosion cracking. By relieving the stress caused by initial stage of annealing able to restore the alloy's toughness. Dislocation density of work harden alloys reduces through this annealing. Subsequent fall of impact energy for all the alloys are attributed to formation of intermetallic like GP zones and metastable phases. These intermetallics make obstruction to dislocation motion in between particles spacing. High temperature also caused grain coarsening and the dissolution of the intermetallic phase, which both added to the toughness value of pure aluminum and aluminum alloys. The dissolution of the different intermetallic phases takes place at different temperature so the intensity and position of the curves is different. However, new grains at high temperatures are often responsible for a decrease in toughness in certain circumstances [26].

Optical microstructures

Fig. 7 shows the obtained microstructure of the 80 % cold rolled experimental alloys at room temperature. It is clearly seen that cold rolling has deformed the grains, resulting in elongated grains in the rolling direction. Except the pure 1xxx series Al alloy the grain boundary is thick because of different alloying elements present there. The intermetallic complexes are disrupted by the rolling effect throughout the alloy causing it to be crushed and clustered at the grain boundaries for 3xxx, 4xxx, and 5xxx alloys. Mg-added 5xxx alloy, on the other hand, has more clustered particles at the grain boundary. As magnesium caused corrosion cracking in the aluminum alloy, the corroded particles were also crushed and began to accumulate at the grain boundaries. Because of the deformed grains and intermetallic particles, all of the alloys experienced an increase in

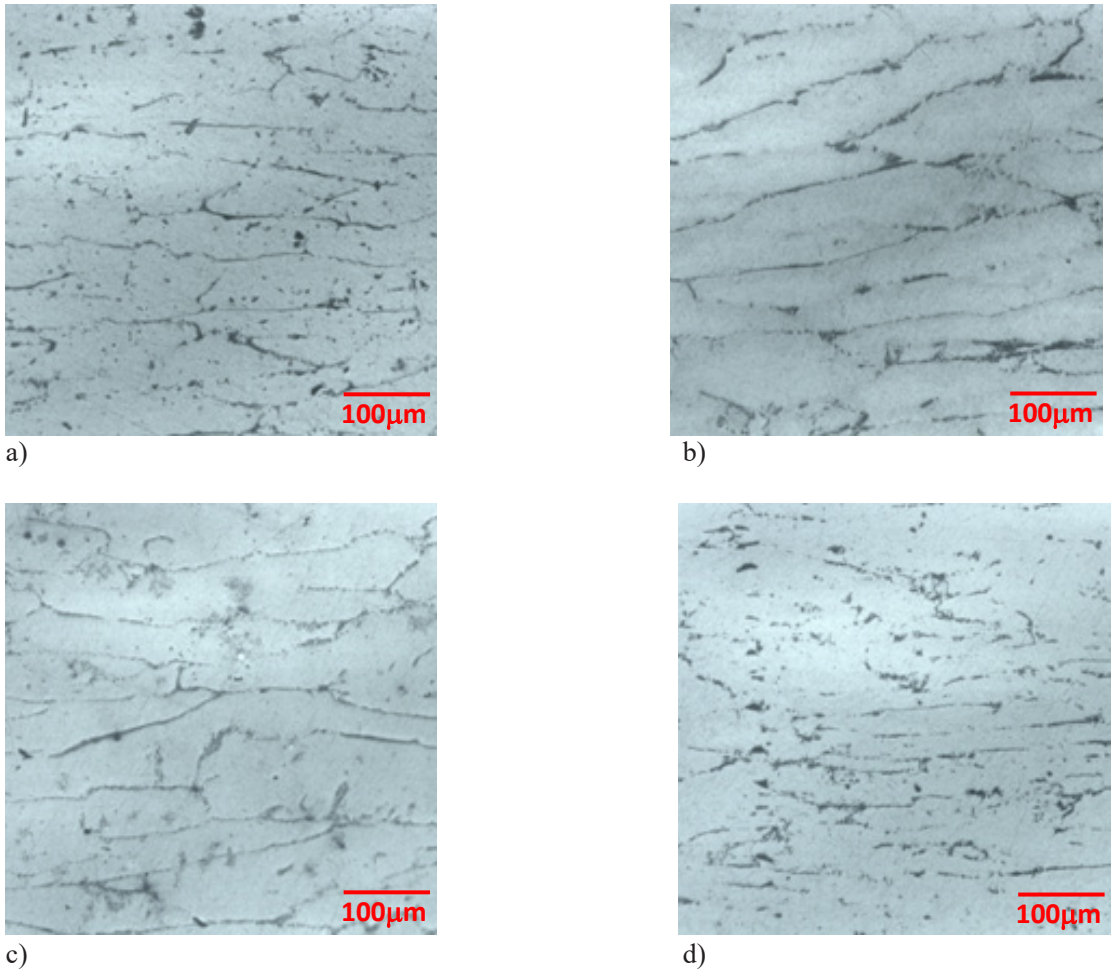

a) b) c) d)

Fig. 7. Optical microstructure of hot and cold rolled: a) 1xxx, b) 3xxx c) 4xxx and d) 5xxx alloys.

their micro hardness and resistivity [27].

Fig. 8 is a representation of the material's microstructure after it had been subjected to a heat treatment at a temperature of 400°C for one hour. Since the intermetallic complex dissolves at higher temperatures, the number of intermetallic compounds along the grain boundary drops. The formerly elongated and distorted grains are absent. However, after an hour of annealing at 400°C, most of the intermetallic compounds in 5xxx alloy had been highly dissolved because of lower dissolution temperature. On the other hand, higher dissolution temperature cases the lower dissolved of second phases in case of Mn added alloy. However, Si added alloy shows the fine distribution of the particles defused from the Al matrix. In case of commercially pure Al indicated the lower second phase, it contents the minimum elements as an impurity and the grains of all alloy has partially recrystallized [29].

Fracture behavior

The SEM fractography depicted in Fig. 9 was taken from a variety of various series of aluminum alloys that were first hot rolled and then 80 % cold rolled. The samples were also subjected to a tensile test at a strain rate of 10^{-3}/s after being annealed at 150°C for an hour. Large dimples and voids of varying sizes are visible in commercially pure Al of the 1xxx series, which may be indicative of ductile fracture and secondary fractures were also identified on the fractured blocks (Fig. 9(a)). Meanwhile, the dimple size is getting smaller, suggesting a mixed mode of fracture, in alloys with Mn, Si, and Mg added to the 3xxx, 4xxx, and 5xxx series, respectively (Fig. 9(b), 9(c), and 9(d)). These elements hamper the grain growth during solicitation. The Mn-added

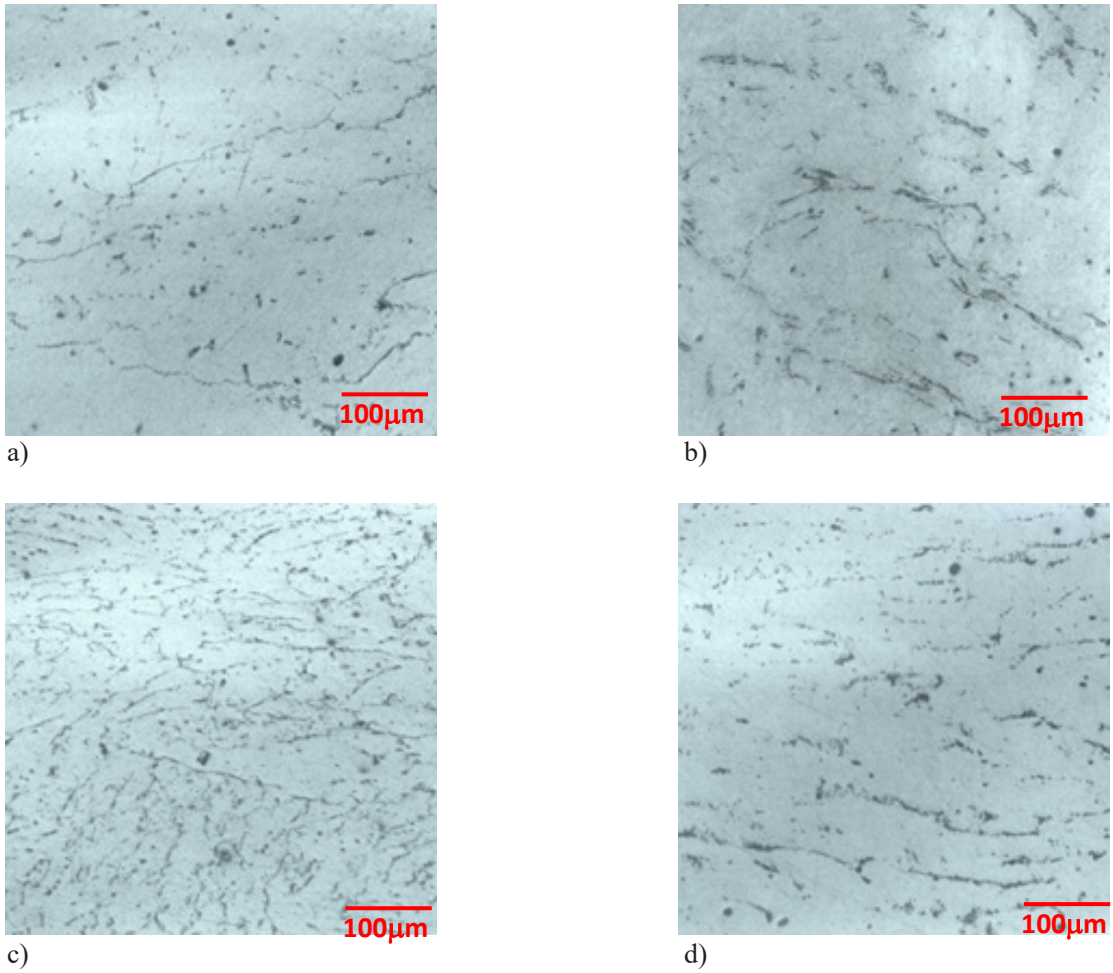

a) b) c) d)

Fig. 8. Optical microstructure of: a) 1xxx, b) 3xxx, c) 4xxx and d) 5xxx alloys annealed at 400°C for one hour.

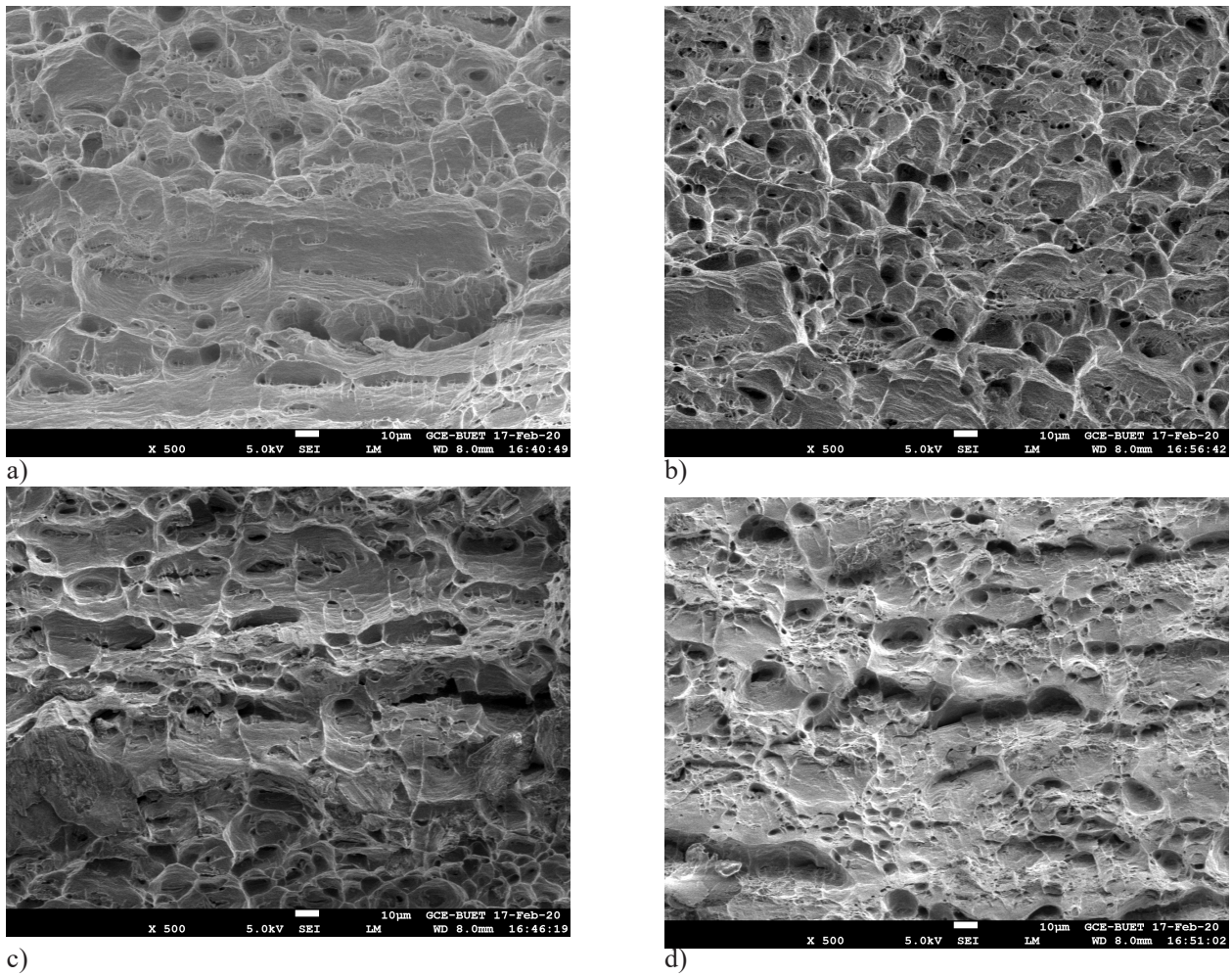

Fig. 9. SEM fractography of tensile surface of: a) 1xxx, b) 3xxx, c) 4xxx and d) 5xxx alloys annealed at 150°C for one hour.

alloy retains fine dimples with a much larger cleavage surface. It is well known that 3xxx alloys contain the intermetallic $Al_{12}Mn$ that could cause cracks to occur [30]. The continuous distribution of brittle, eutectic and globular Si particles in the 4xxx alloy initiated the crack and offered an easier path for crack propagation, which led to the observation of considerably larger cleavage surface in the 4xxx alloy than in the 3xxx and 5xxx alloys. Debonding or fracturing of Si particles at the Al/Si contact causes fracture to propagate preferentially along the boundaries between the Al matrix and the Si particles in the matrix. The addition crack produced by the Al_3Mg_2 intermetallic via stress corrosion cracking is readily seen on the fracture surface of 5xxx series alloy. Furthermore, there is a significant amount of spherical particles dispersed throughout the bottom and wall of the little dimples. These fragments are the result of brittle precipitates breaking apart, proving that the material has experienced inter-granular fracture. As a result, 3xxx, and 5xxx alloys break using a combination of ductile and brittle mechanisms [31, 32].

CONCLUSIONS

This study was concerned with the effect of alloying elements on the strengthening process of non-heat-treatable aluminum alloys by solid solution strengthening and post-deformation annealing. These findings are based on considerable experimental analysis.

- The commercially pure 1xxx series Al-alloy offers the minimum strength followed by Si added 4xxx, Mn added 3xxx alloy and the highest for Mg added 5xxx series alloy as accredited to the alloying element performance. Increase in annealing temperature minimal of dislocation density, recovery, particle coarsening and recrystallization process leading to a

decrease in hardness and resistivity of the non-heat treatable alloys. As a result, the true stress - strain curves show the declined in nature, lower strength and higher elongation with higher annealing temperature.

- Cold rolled alloys 3xxx, 4xxx and 5xxx series Al-alloys contents the elongated grain with thick grain boundary because of elements adding together except 1xxx series pure Al-alloy. The recrystallized grain is formed when the alloys are annealed at 400°C for one hour as dismiss the elongated grains.
- Commercially pure aluminum 1xxx series Al-alloy exhibits the fully ductile fracture but manganese added 3xxx and magnesium added 5xxx series alloys consist of some brittle fracture as they form intermetallics. In case of Si added 4xxx alloy consists of ductile fracture but initiated by the eutectic and globular Si particles.

Acknowledgements

The authors would like to thank the DAERS office at the Bangladesh University of Engineering and Technology located in Dhaka-1000, Bangladesh for their assistance with this study. The corresponding author would like to express his gratitude towards the Director Administration of IUBAT, for her efforts in fostering collaborations with other institutions have also been commendable.

REFERENCES

1. I. Polmear, D.S. John, J.F. Nie, M. Qian, Light Alloys Metallurgy of the Light Metals, 5th Edition, Butterworth-Heinemann Elsevier Ltd, Oxford, UK, 2017.
2. T. Lee, Resistance spot weldability of heat-treatable and non-heat-treatable dissimilar aluminium alloys, Science and Technology of Welding and Joining, 25, 7, 2020, 543-548.
3. C.H. Ng, S.N.M. Yahaya, A.A.A. Majid, Reviews on aluminum alloy series and its applications, Academia Journal of Scientific Research, 5, 12, 2017, 708-716.
4. M.E. Shennawy, K.A. Aziz, A.A. Omar, Metallurgical and Mechanical Properties of Heat Treatable Aluminum Alloy AA6082 Welds, International Journal of Applied Engineering Research, 12, 11, 2017, 2832-2839.
5. M.S. Kaiser, Effect of Solution Treatment on Age-Hardening Behavior of Al-12Si-1Mg-1Cu Piston Alloy with Trace-Zr Addition, Journal of Casting & Materials Engineering, 2, 2, 2018, 3037.
6. J. Torzewski, M. Lazinska, K. Grzelak, I. Szachogłuchowicz, J. Mierzynski, Microstructure and Mechanical Properties of Dissimilar Friction Stir Welded Joint AA7020/AA5083 with Different Joining Parameters, Materials (Basel), 15, 5, 2022, 1-16.
7. M.S. Kaiser, Precipitation and softening behaviour of cast, cold rolled and hot rolling prior to cold rolled Al-6Mg alloy annealed at high temperature, Journal of Mechanical Engineering, 45, 1, 2015, 32-36.
8. D. Varshney, K. Kumar, Application and use of different aluminium alloys with respect to workability, strength and welding parameter optimization, Ain Shams Engineering Journal, 12, 1, 2021, 1143-1152.
9. J. Zheng, Q. Pang, Z. Hu, Q. Sun, Recent Progress on Regulating Strategies for the Strengthening and Toughening of High-Strength Aluminum Alloys, Materials, 15, 13, 2022, 1-30.
10. M.S. Kaiser, S. Datta, A.R. Chowdhury, M.K. Banerjee, Age Hardening Behavior of Wrought Al–Mg–Sc Alloy, Materials and Manufacturing Processes, 23, 1, 2008, 74-81.
11. R. Hu, C. Guo, M. Ma, A Study on High Strength, High Plasticity, Non-Heat Treated Die-Cast Aluminum Alloy, Materials, 15, 295, 2022, 1-14.
12. X. Zhu, F. Liu, S. Wang, S. Ji, The development of low-temperature heat-treatable high-pressure die-cast Al–Mg–Fe–Mn alloys with Zn, Journal of Materials Science, 56, 2021, 11083-11097.
13. R.E. Sanders J.P.A. Hollinshead, E.A. Simielli, Industrial Development of Non-Heat Treatable Aluminum Alloys, Materials Forum, 28, 2004, 53-64.
14. M.S. Kaiser, H.M. M. A. Rashed, Precipitation behavior prior to hot roll in the cold-rolled Al-Mg and Al-Mg-Zr alloys, Kovove Materialy, 60, 4, 2022, 247-256.
15. M. Mhedhbi, M. Khlif, C. Bradai, Investigations of microstructural and mechanical properties evolution of AA1050 alloy sheets deformed by cold-rolling process and heat treatment annealing, Journal of Materials and Environmental Science, 8, 8, 2017, 2967-2974.

16. G. Eriksson, A.D. Pelton, Critical evaluation and optimization of the thermodynamic properties and phase diagrams of the MnO-TiO_2, MgO-TiO_2, FeO-TiO_2, Ti_2O_3-TiO_2, Na_2O-TiO_2, and K_2O-TiO_2 systems, Metallurgical Transactions B, 24, 1993, 795-805.
17. X. Liu, I. Ohnuma, R. Kainuma, K. Ishida, Thermodynamic assessment of the Aluminum-Manganese (Al-Mn) binary phase diagram. Journal of Phase Equilibria, 20, 1, 1999, 45-56.
18. S. Ikhmayies, Phase Diagrams of Al–Si System, Conference proceedings, Energy Technology, 2019, 231-237.
19. M.S. Haque, S.A. Khan, M.S. Kaiser, Effect of Sc and Zr on Precipitation Behaviour of Wrought Al-Bronze, IOP Conference Series: Materials Science and Engineering, 1248, 1, 2022, 012037.
20. D. Chen, C. You, F. Gao, Analysis and Experiment of 7075 Aluminum Alloy Tensile Test. Procedia Engineering, 81, 2014, 1252-1258.
21. M. Jain, J. Allin, D. Lloyd, Fracture limit prediction using ductile fracture criteria for forming of an automotive aluminum sheet, International Journal of Mechanical Sciences, 41, 10, 1999, 1273-1288.
22. V. Hoa, D. Seo, J. Lim, Site of ductile fracture initiation in cold forging: A finite element model. Theoretical and Applied Fracture Mechanics, 44, 1, 2005, 58-69.
23. G. Beck, K. Petrikowski, Influence of the microstructure of the aluminum substrate on the regularity of the nanopore arrangement in an alumina layer formed by anodic oxidation, Surface and Coating Technology, 202, 21, 2008, 5084-5091.
24. K. Skibinska, G. Smola, L. Bialo, D. Kutyla, K. K. Siedlecka, A. Kwiecinska, M. Wojnicki and P. Zabinski, Influence of Annealing Time of Aluminum AA1050 on the Quality of Cu and Co Nanocones, Journal of Materials Engineering and Performance, 29, 12, 2020, 8025-8035.
25. E.J. Hearn, Mechanics of Materials, 3rd Edition, Butterworth-Heinemann, Oxford, UK, 1997.
26. I. Uytdenhouwen, M. Decréton, T. Hirai, J. Linke, G. Pintsuk, G.V. Oost, Influence of recrystallization on thermal shock resistance of various tungsten grades. Journal of Nuclear Materials, 363-365, 2007, 1099-1103.
27. V. Auradi, M.S. Prabhudev, V. Karodi, N.H. Siddalingswamy, S.A. Kori, Influence of Cu addition on dry sliding wear behaviour of A356 alloy, Procedia Engineering, 97, 2014, 1361-1367.
28. T. Furu, R. Rsund, E. Nes, Substructure evolution during different hot deformation processes of commercial non-heat treatable aluminium alloys. Materials Science and Engineering: A, 214, 1-2, 1996, 122-132.
29. Z. Kotsina, A. Theodorou, E. Mitsi, M. Axiotis, G. Apostolopoulos, The effect of recrystallization on the resistivity recovery of W, Journal of Nuclear Materials, 558, 2022, 153368.
30. J. Rawers, K. Perry, Crack initiation in laminated metal-intermetallic composites, Journal of Materials Science, 31, 13, 1996, 3501-3506.
31. C. Yin, D. Terentyev, T. Pardoen, R. Petrov, Z. Tong, Ductile to brittle transition in ITER specification tungsten assessed by combined fracture toughness and bending tests analysis, Materials Science and Engineering: A, 750, 2019, 20-30.
32. M. Jetter, J. Aktaa, Probabilistic analysis of cleavage fracture in commercial polycrystalline tungsten, Journal of Nuclear Materials, 565, 30, 2022, 153757.